


# Palaeoenvironmental history of the last six centuries in the Nettilling Lake area (Baffin Island, Canada): A multi-proxy analysis

The Holocene  
2016, Vol. 26(11) 1835–1846  
© The Author(s) 2016  
Reprints and permissions:  
sagepub.co.uk/journalsPermissions.nav  
DOI: 10.1177/0959683616645937  
hol.sagepub.com  


Anne Beaudoin,<sup>1</sup> Reinhard Pienitz,<sup>1,2</sup> Pierre Francus,<sup>2,3</sup>  
Christian Zdanowicz<sup>4</sup> and Guillaume St-Onge<sup>5</sup>

## Abstract

The Baffin Island region in the eastern Canadian Arctic has recently experienced a rapid warming, possibly unprecedented in millennia. To investigate the response of freshwater environments to this warming and place it in a secular perspective, we analyzed a 90-cm-long sediment core from Nettilling Lake, the largest lake of the Canadian Arctic Archipelago. The core was taken from a part of the lake basin that receives meltwater and sediment inputs from the nearby Penny Ice Cap. The core time scale, established using <sup>137</sup>Cs and palaeomagnetic techniques, spans an estimated 600 years. A multi-proxy approach was used to document changes in the physical, chemical, and biological properties of the sediments. We found evidence for a relatively warm period (mid/late 15th century to mid/late 16th century) during the early part of the 'Little Ice Age' (LIA), characterized by high sedimentation rates and laminations. This was followed by colder, drier, and windier conditions corresponding to the coldest phase of LIA and coinciding with the latest and most extensive period of regional ice cap expansion (early 16th to late 19th centuries). A rapid warming occurred at the beginning of the 20th century. Variations in titanium (Ti) content in the core, a proxy for detrital sediment inputs, showed good agreement with reconstructed secular variations in summer melt rates on Penny Ice Cap between the mid-14th century and the present-day, providing supporting evidence for a climatic–hydrological connection between the ice cap and Nettilling Lake.

## Keywords

Baffin Island, lake sediments, 'Little Ice Age' environment interaction, Nettilling Lake, palaeoclimate, Penny Ice Cap

Received 20 November 2014; revised manuscript accepted 29 February 2016

## Introduction

High latitude ecosystems are particularly vulnerable to impacts of recent human-induced climate change due to numerous positive feedback mechanisms (Everett and Fitzharris, 1998; Overpeck et al., 1997). Earlier spring snowmelt and declining lake and sea-ice cover extents, associated with decreasing surface albedo, result in increased exposure to, and absorption of, solar energy. Observed and predicted consequences of climate warming at high latitudes include higher air temperatures, modifications of the hydrological regime, permafrost degradation, and melting of glaciers and ice caps (Pienitz et al., 2004).

Evidence of recent warming in the Foxe Basin/southern Baffin Island region (Miller et al., 2013) includes a reduction in seasonal sea ice cover volume (Moore, 2006) and an increased rate of summer melting on terrestrial ice caps (Zdanowicz et al., 2012). Long instrumental climate records in the Canadian Arctic are very sparse. In the absence of such records, pollen, diatoms or other lake sediment properties can be used to reconstruct regional climate variations or the response of aquatic ecosystems to these variations. In particular, lakes are known to respond rapidly to environmental changes, such as variations in temperature (e.g. Pienitz et al., 2004). An increase of only a few degrees can profoundly change ice cover conditions, modify the lake dynamics, and increase primary productivity (Hodgson and Smol, 2008; Wolfe and Smith, 2004). Numerous studies have shown that recent environmental changes experienced by northern lakes are without any analogues throughout the Holocene and beyond (e.g. Axford et al., 2009; Wolfe and Smith, 2004).

Nettilling Lake on south-central Baffin Island has the largest freshwater catchment in the Canadian Arctic Archipelago and, as such, is an interesting study site for understanding the impact of current climate change on Arctic lacustrine environments. In this paper, we present the first detailed reconstruction of the past

<sup>1</sup>Laboratoire de paléocéologie aquatique (LPA), Département de Géographie and Centre d'études nordiques (CEN), Université Laval, Canada

<sup>2</sup>Centre Eau Terre Environnement (ETE), Institut national de la recherche scientifique (INRS), Canada

<sup>3</sup>Centre d'études nordiques (CEN), Université Laval, Canada

<sup>4</sup>Department of Earth Sciences, Uppsala University, Sweden

<sup>5</sup>Institut des sciences de la mer de Rimouski (ISMER), Canada Research Chair in Marine Geology, Université du Québec à Rimouski and GEOTOP Canada

## Corresponding author:

Anne Beaudoin, Laboratoire de paléocéologie aquatique (LPA), Département de Géographie and Centre d'études nordiques (CEN), Université Laval, Pavillon Abitibi-Price, 2405 rue de la Terrasse, Québec, QC G1V 0A6, Canada.  
Email: anne.beaudoin.1@ulaval.ca

Reinhard Pienitz, Laboratoire de paléocéologie aquatique (LPA), Département de Géographie and Centre d'études nordiques (CEN), Université Laval, Pavillon Abitibi-Price, 2405 rue de la Terrasse, Québec, QC G1V 0A6, Canada.  
Email: reinhard.pienitz@cen.ulaval.ca



**Figure 1.** Location map with Netting Lake, Penny Ice Cap and surrounding region. Ni5-8 = lake coring site in 2010. Netting Lake watershed limit modified from Jacobs et al. (1997). Ordovician cover extent modified from St-Onge et al. (2007).

environmental history of Netting Lake, developed using an innovative, multi-proxy approach that integrates physical, chemical, and biological properties recorded in lake sediments. Our main goal was to document past environmental and hydro-climatic changes in Netting Lake. In addition, we compared the sedimentary record of Netting Lake with an ice-core-based proxy record of summer warmth developed from nearby Penny Ice Cap (Grumet et al., 2001; Zdanowicz et al., 2012), which supplies abundant meltwater and sediments to the lake.

### Study site

Netting Lake (66.51°N, 70.90°W) is located in the south-central part of southern Baffin Island and has an estimated surface

area of 5542 km<sup>2</sup> (Figure 1). The maximum measured lake water depth is 132 m, but most of the lake is less than 60 m deep (Oliver, 1964). With an estimated catchment area of 52,970 km<sup>2</sup> (including the Amadjuak Lake catchment area), Netting Lake is the most extensive freshwater aquatic drainage system in the Canadian Arctic Archipelago. However, because of its remote location, it has received limited research attention, and little is known of its past environmental history (Jacobs et al., 1997; Oliver, 1964).

Like most Arctic lakes, Netting Lake has a low biological productivity, and its ice cover persists approximately from mid-September to mid-July (Oliver, 1964, and recent observations by the authors, 2010–2015). The lake can be subdivided into two main morphological regions separated by a line from Magnetic Point (south shore) to Caribou Point (north shore);

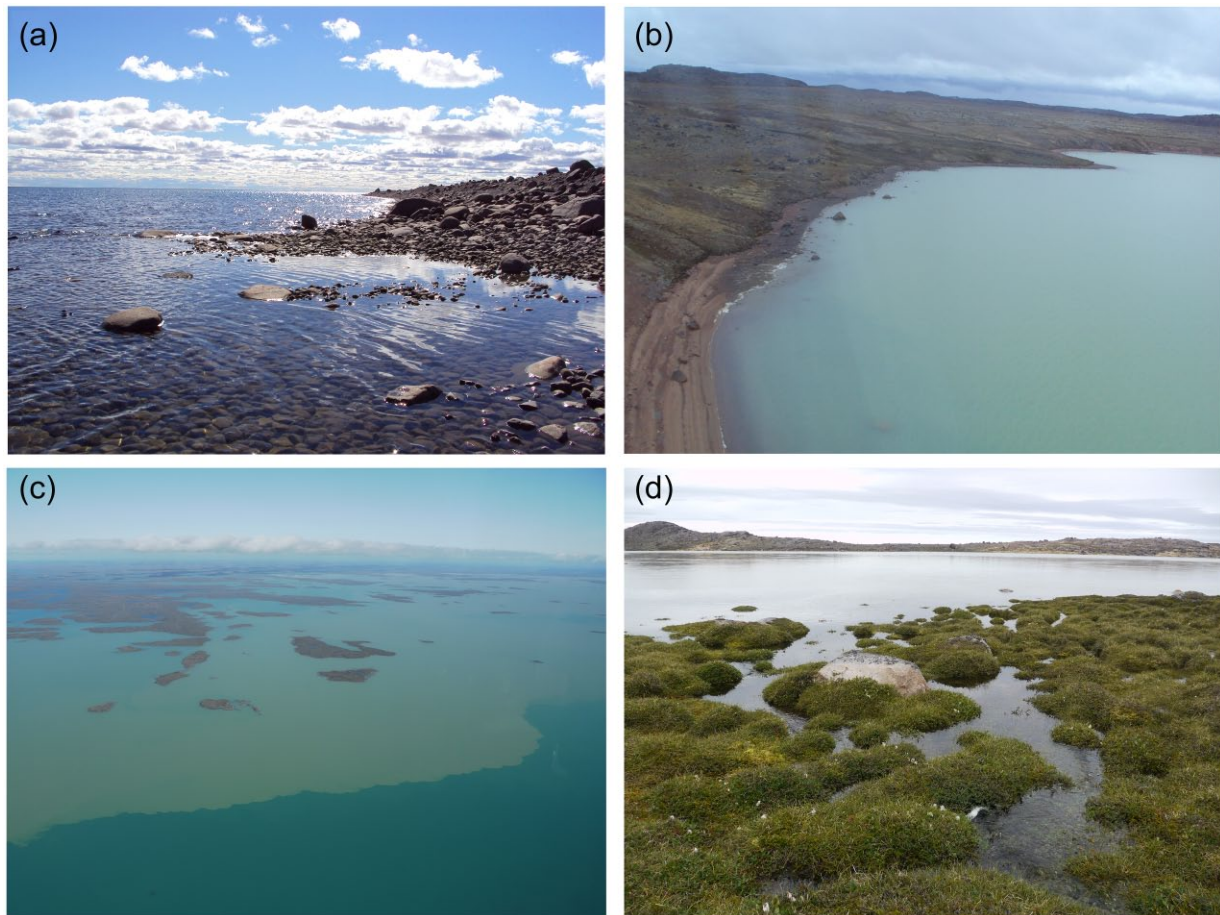


**Figure 2.** (a) Transparent waters of the western part of Nettiilling Lake; (b) inputs of glacial meltwater highly charged with silt in the northeastern part of the lake (photos: Anne Beaudoin, August 2010); (c) plume of sediments in Nettiilling Lake from glacial meltwater highly charged with silt; (d) moss- and sedge-dominated wetlands along the banks of the Isurtuq River, near its inflow into Nettiilling Lake (photos: Reinhard Pienitz, August 2014).

Figure 1). The western region has a regularly shaped deep basin and shoreline, while the eastern region has more irregular basin and shoreline shapes and numerous islands. This subdivision coincides with the contact between two different geological settings: the lowlands on the western side of the lake basin are mostly composed of Palaeozoic carbonates (Hudson Platform), whereas the bedrock of the eastern side is mostly made up of low-relief granite and gneiss plateaus of Precambrian age belonging to the Canadian Shield (Blackadar, 1967). Both areas are covered by unconsolidated glacial drift. Nettiilling Lake is located below the estimated regional maximum postglacial marine transgression limit (~93 m above sea-level (a.s.l.)) and was therefore likely submerged by marine waters of the postglacial Tyrrell Sea about 6.7 ka BP, following the retreat of the Laurentide Ice Sheet (Blake, 1966; Dyke, 1979; Jacobs et al., 1997). The postglacial isostatic rebound eventually isolated the area from marine influence and allowed the establishment of a freshwater basin around 5 ka BP (Blake, 1966; Narancic et al., 2013).

Nettiilling Lake drains to the west into Foxe Basin via the large Koukdjuak River (~74 km long) (Figure 1). Main tributaries feeding into Nettiilling Lake are Amadjuk Lake, located to the south, and the Isurtuq River to the northeast. Isurtuq River, which is fed by meltwater from Penny Ice Cap, is about 235 km long and splits into two channels about 7 km before entering into Nettiilling Lake. Together, these hydrographic features have and probably continue to exert influence on sediment delivery into Nettiilling Lake.

Penny Ice Cap (6410 km<sup>2</sup>) is a remnant of the Foxe Dome sector of the Wisconsinan Laurentide Ice Sheet (Fisher et al., 1998). Summer melt rates on the ice cap have been increasing irregularly since the mid-19th century, with the most recent acceleration after

the 1980s, and are presently as high as they have ever been through the Late-Holocene (Zdanowicz et al., 2012). Inputs of glacial meltwater from Penny Ice Cap, highly charged with silt, create a large plume of suspended material in the eastern part of Nettiilling Lake, which contrasts with the transparent waters of the western basin (Figure 2).

## Materials and methods

### Sediment core collection

Field work was conducted at Nettiilling Lake during the summer of 2010. In this paper, we focus on results obtained from core Ni5-8, a 90-cm-long core retrieved with a percussion corer at a water depth of 18.9 m in a small bay in the northeastern part of the lake (66.67°N, 69.92°W) (Figure 1), using a handheld percussion corer (Aquatic Research Instruments). The maximum thickness of the sediments deposited at this site is presently unknown. The sampling site was chosen based on its location near the outlet of Isurtuq River, which provides favorable setting for the preservation of a climatically modulated record of detrital inputs from Penny Ice Cap glacial meltwater.

### Core analysis

**Sedimentology and chemical analyses.** In the Laboratoire de paléocéologie aquatique (LPA) at Université Laval, one half of core Ni5-8 was sampled at 0.5 cm resolution and then freeze-dried during 48 h. Organic matter (OM) content was determined at 1 cm resolution (one sample out of two) on 0.3 g of dry sediment using

loss-on-ignition (LOI) at 550°C during 5 h, following the method of Heiri et al. (2001). Grain size analyses were performed at 1 cm resolution using a HORIBA laser diffraction analyzer at the Laboratoire de géomorphologie et sédimentologie at Université Laval. About 0.3 g of freeze-dried sediment (OM removed by combustion) was mixed in 5 mL of calgon electrolytic solution (hexameta-phosphate, 10%). Prior to grain size measurements, each sample was exposed to ultrasound for 2 min in order to break down aggregates. Statistical parameters of the grain size distribution (mean, median, skewness, and sorting) were then calculated with the GRADISTAT v8.0 software using the geometric method of moments (Blott and Pye, 2001).

The remaining half-sectioned core was first analyzed for magnetic susceptibility at the Institut des sciences de la mer de Rimouski (ISMER) of the Université du Québec à Rimouski. Measurements were done every centimeter using a Bartington point sensor on a GEOTEK multi-sensor core logger. The same half-sectioned core was then analyzed for major and minor element geochemistry using an ITRAX core scanner at the Institut national de la recherche scientifique, Centre Eau Terre Environnement (INRS-ETE), Québec. This instrument uses x-ray fluorescence (XRF) to measure semi-quantitative fluctuations in geochemical elemental abundances (Croudace et al., 2006). Measurements were done at high-resolution intervals (100 µm with 30 s of exposure time, 30 kV of voltage and 25 mA of current) using a molybdenum-source x-ray tube, and individual elemental profiles (in counts per seconds; cps) were normalized by the total counts (expressed in kcps) at the corresponding depths to eliminate the effects of variable water and OM content in the sediment core (Croudace et al., 2006). Profiles were smoothed with a running mean over 1000 µm intervals. The scanner also produces a positive x-ray radiograph (a proxy for core density) with a 100 µm resolution.

Thin sections of core Ni5-8 were made according to methods described in Lamoureux (1994) to characterize and interpret the fine sedimentary structures. Slabs of sediment (18 cm long × 2 cm wide × 0.7 cm deep) were sampled, submerged in liquid nitrogen, and then freeze-dried for 48 h. Samples were impregnated in a low viscosity resin under light vacuum. After 48 h in an oven at 80°C, slabs were cut with a 45° angle into three blocks, from which polished thin sections were prepared.

**Dating.** In order to construct a depth–age model for core Ni5-8, two different approaches were combined: radiometric dating and palaeomagnetism. First, the cesium-137 (<sup>137</sup>Cs) activity of the sediment was measured in the top 30 cm of core Ni5-8 by gamma-ray spectroscopy using a High Purity Germanium (HPGe) well detector system at the Laboratoire de radiochronologie, Université Laval. The measurements were carried out at 1 cm intervals from 0 to 30 cm depth. Radiocarbon (<sup>14</sup>C) and lead 210 (<sup>210</sup>Pb) measurements were also performed, but results were not considered usable because of extremely low OM content and the predominance of sediment probably eroded from the crystalline bedrock beneath Penny Ice Cap (see supplementary file, available online).

To develop the depth–age model beyond 15 cm core depth, we combined <sup>137</sup>Cs and palaeomagnetism. This method is based on the principle that, under favorable conditions in aquatic environments, magnetic particles in the sediments can record the orientation and intensity of the geomagnetic field at the time of deposition (e.g. Stoner and St-Onge, 2007; Tauxe, 2010), which can also be estimated from geomagnetic models (e.g. Korte and Constable, 2011). To measure changes in direction of the geomagnetic field, magnetic properties were measured at 1 cm intervals at the Laboratoire de paléomagnétisme et géologie marine of ISMER (Rimouski, Québec), using a 2 G Enterprises™ 755 cryogenic magnetometer on three U-channels (4 cm<sup>2</sup>). Because the core had

been already subsampled for thin sections, a few sections of the U-channels were not completely filled with sediment. To minimize errors in measurements, U-channels were overlapped and data were removed from the dataset where duplication of U-Channel sampling intervals was not possible (gaps in Figure 3). The Natural Remanent Magnetization (NRM) was measured using alternating field (AF) demagnetization steps from 0 to 75 mT (5 mT increments). The magnetic inclination in the sediment was computed by principal component analysis (PCA) using AF demagnetization steps from 15 to 75 mT (Mazaud, 2005). The maximum angular deviation (MAD) values were also computed and used as indicators of the quality of the palaeomagnetic data.

**Biological analyses.** In the LPA, fossil diatoms preserved in core Ni5-8 were extracted with hydrogen peroxide (30% H<sub>2</sub>O<sub>2</sub>) digestion techniques and mixed with marker microspheres (1.57 × 10<sup>6</sup> microspheres ml<sup>-1</sup>). Microscope slides were mounted using *Naphrax*, a highly refractive synthetic resin (Battarbee et al., 2002). A minimum of 300–500 diatom valves were counted and identified for each subsample according to their concentration. Where diatoms were less abundant, 300 valves were identified or 1000 microspheres were counted. Identification of diatom species was made using a Leica DMRB microscope at 1000× magnification under oil immersion. The main taxonomic keys used were Fallu et al. (2000), Krammer and Lange-Bertalot (1986, 1988, 1991a, 1991b), and Antoniadès et al. (2008).

**Statistical analyses.** Chronological cluster analysis was performed on down-core profiles of normalized chemical element abundances, LOI, and water content to detect common patterns of variations in these data. Data were first standardized and transformed in Euclidean distance, and the clustering results were used to divide core Ni5-8 into distinct stratigraphic zones. The number of significant zones was determined using the broken stick model (Birks, 2012). Geochemical data were transformed from depth (cm) to age (year) scale using the developed age model (see section ‘Stratigraphy and sedimentology’) in order to facilitate comparisons with other records. Correlation coefficients (*R*) between different profiles of chemical elements were computed on the normalized data. Serial autocorrelations in the data were taken into account, and reduced degrees of freedom were used in order to test the significance of the observed correlations (Ebisuzaki, 1997).

## Results

### Development of core chronology

The chronology of core Ni5-8 was developed using <sup>137</sup>Cs and palaeomagnetic secular variations (PSV) correlated with geomagnetic field model outputs. Such a combination of techniques has been successfully applied for dating marine and lake sediments at other sites in the Canadian Arctic (e.g. Antoniadès et al., 2011; Barletta et al., 2010a; Cook et al., 2009; St-Onge and Stoner, 2011). The <sup>137</sup>Cs profile presents a well-defined peak at 6.25 cm, which is attributed to the year AD 1963 when maximum atmospheric fallout of <sup>137</sup>Cs from pre-moratorium surface nuclear weapon tests was attained (Figure 3a) (Appleby, 2001). The <sup>137</sup>Cs peak is sharp, which suggests negligible vertical mixing in the sediments.

Geomagnetic inclination variations were used to define the core chronology below 15 cm depth (Figure 3). Inclination values oscillate around the geocentric axial dipole (GAD) (77.8°N for Nettilling Lake) and very low MAD values were obtained (below 5.4°, with a mean of 2.3°), which indicate high-quality directional data (Stoner and St-Onge, 2007). An initial chronology was first developed for the entire core Ni5-8 assuming a constant sedimentation rate based on <sup>137</sup>Cs peak. The inclination profile was then

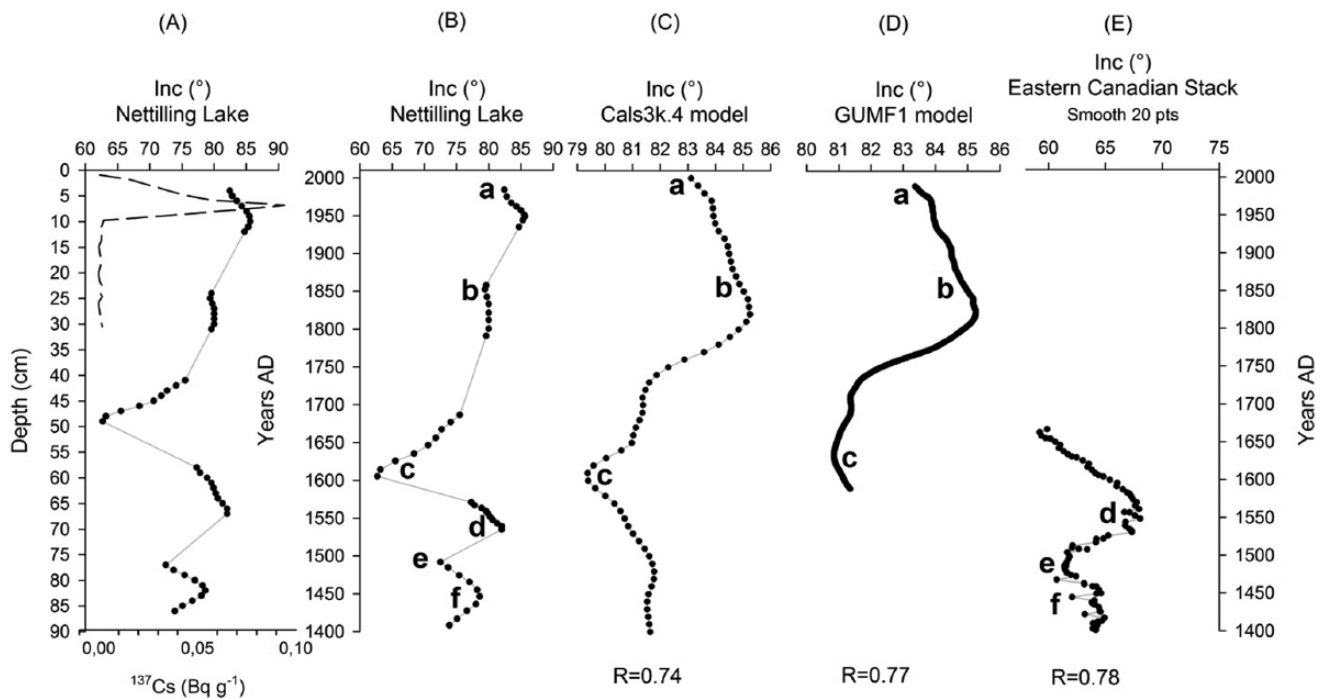


**Figure 3.** Comparison of (a and b) palaeomagnetic inclination records from the Nettilling Lake core Ni5-8; dashed line =  $^{137}\text{Cs}$  activity, (c) output from the CALS3k.4 model for this region (Korte and Constable, 2011), (d) output of the GUMF1 model (Jackson et al., 2000), and (e) the Eastern Canadian Stack (Barletta et al., 2010b).

**Table 1.** Correlated tie points with the Cals3k.4 (Korte and Constable, 2011), GUMF1 (Jackson et al., 2000) models and the Eastern Canadian stack (Barletta et al., 2010b) associated with depth in core Ni5-8.

	Cals3k.4	GUMF1	Eastern Canadian stack	Estimated mean age (AD)	Depth (cm)
a	1980	1984	–	1982	4
b	1850	1842	–	1846	25
c	1610	1625	–	1617.5	49
d	–	–	1541	1541	66
e	–	–	1492	1492	77
f	–	–	1450	1450	82

compared with several model reconstructions of past global geomagnetic field variations for the location of Nettilling Lake using the AnalySeries 2.0.4 software (Paillard, 2006) to provide further chronological constraints (Figure 3). We used the Cals3k.4 model that spans the past 3000 years (Korte and Constable, 2011), as well as the GUMF1 model which extends back to AD 1590 (Jackson et al., 2000). In addition, we compared the Ni5-8 inclination record with the Eastern Canadian Stack, a  $^{14}\text{C}$ -constrained compilation of marine palaeomagnetic directional and palaeointensity records (Barletta et al., 2010b).

Correlations between the Ni5-8 palaeomagnetic profile and these various datasets were established using six tie points labeled a to f in Figure 3 and Table 1. A highly significant correlation was found between the Ni5-8 inclination series and the Cal3k.4 model output for the Nettilling Lake region ( $R=0.74$ ,  $p=0.0147$ ,  $\alpha=0.05$ ). The inclination profile of core Ni5-8 was also highly correlated with the GUMF1 model for the region ( $R=0.77$ ,  $p\leq 0.01$ ,  $\alpha=0.05$ ).

The age–depth model developed by combining  $^{137}\text{Cs}$  and palaeomagnetic data gives an estimated bottom age for core Ni5-8 in the early 14th century, at AD~1362 (Figure 4). The time interval recorded in core Ni5-8 therefore spans much or most of the ‘Little Ice Age’ (LIA) cold climate interval, which, on the basis of various palaeoclimatic proxies, is estimated to have lasted from the

mid/late 13th to the 19th century in the eastern Canadian Arctic (Briner et al., 2009; Grumet et al., 2001; Kaufman et al., 2009; Margreth et al., 2014; Miller et al., 2012; Moore et al., 2001; Rolland et al., 2009; Thomas and Briner, 2009).

Our age–depth model for core Ni5-8 yields sedimentation rates ranging from 0.10 to 0.26  $\text{cm a}^{-1}$  over the past ~600 years, with an average of 0.15  $\text{cm a}^{-1}$ , close to the one (0.13  $\text{cm a}^{-1}$ ) obtained from the  $^{137}\text{Cs}$  peak.

In order to estimate the possible error of the age model for Nettilling Lake core Ni 5-8, a Markov chain Monte Carlo procedure was employed to simulate stochastic variations in sedimentation rates between pairs of chronostratigraphic markers. The method adopted here shares similarities with the Bayesian approach of Blaauw and Christen (2011), but differs in some respects. In Blaauw and Christen’s method, sedimentation is assumed to follow an autoregressive gamma function, the parameters of which must be estimated *a priori*. In our approach, rather than imposing a defined probability function (PDF), we used Holocene sedimentation data series from proglacial lakes on Baffin Island as models, based on the assumption that sedimentation in Nettilling Lake shares the same type of PDF (whatever it may be) and spectra of temporal variations. Such assumptions are plausible, even if sedimentation rates differ between lakes. The template data used originate from Donard Lake on southeastern Baffin Island (Moore

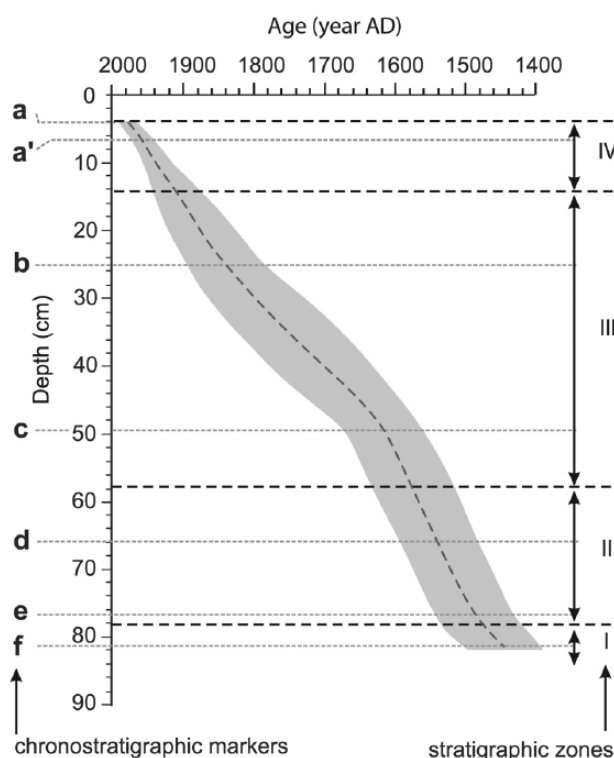


**Figure 4.** Age–depth model for core Ni5-8, constructed using chronostratigraphic markers identified using  $^{137}\text{Cs}$  and the palaeomagnetic inclination curve (Table 1). The broken line is the median age estimate and the gray shading the corresponding 95% confidence bounds, as determined using a Markov chain Monte Carlo procedure. Letters at left identify chronostratigraphic markers (Table 1: a' = 1963  $^{137}\text{Cs}$  bomb layer). Numbers at right denote stratigraphic zones (I–IV) defined by distinctive sedimentological and geochemical variations (see text).

et al., 2001) and from Big Round Lake on northeastern Baffin Island (Thomas and Briner, 2009). In an iterative procedure, randomly selected subsets of these data were used to generate surrogate series of stochastic sedimentation rate variations with the same PDF and temporal spectra as the template series, but with different (prescribed) means. The Iterative Amplitude Adjusted Fourier Transform (IAAFT) algorithm of Schreiber and Schmitz (1996) was used to generate thousands of surrogate series, from which the possible range of corresponding ages between chronostratigraphic markers was estimated. The procedure implicitly takes into account autocorrelation in the data series to the extent that it partly defines their temporal spectra. We also accounted for the possible age uncertainties on the various marker horizons, which were conservatively estimated to range between  $\pm 20$  years ( $2\sigma$ ) for the  $^{137}\text{Cs}$ -dated 1963 layer and  $\pm 50$  years ( $2\sigma$ ) for marker horizons dated by palaeomagnetism. In the latter case, the age uncertainty reflects possible errors in the estimated correlative depths with the Cals3k.4 or GUMFI models, or with the Eastern Canadian Stack, or  $^{14}\text{C}$  uncertainties in the data used to constrain these models. The resulting estimated error range for the age model of core Ni 5-8, as determined by the procedure described above, is shown as gray shading in Figure 4. The width of the shaded envelope corresponds to the outer bounds of the 95% confidence interval, and the broken line is the median age estimate of the sediment layers. The largest dating error, found at mid-depth between horizons b and c ( $\sim 38$  cm), is estimated to be  $\pm 110$  years.

### Stratigraphy and sedimentology

**General core description.** Visual and x-ray examination of core Ni5-8 revealed diffuse, dark yellowish brown layers (Munsell

color scale = 10YR 4/6) and dark gray  $\sim 0.5$ -cm-thick layers (10YR 4/1) in the upper part of the core. A notable perturbation in sedimentary structures (very diffuse layer boundaries) was found in the middle part of the core ( $\sim 17$ – $47$  cm). The lower part (60–90 cm) is also characterized by several black diffuse layers ( $\sim 2$ – $5$  mm). Neither discontinuities nor erosion surfaces were observed in thin sections and x-radiographies.

The lithostratigraphy of core Ni5-8 was divided into four zones of distinctive sedimentological and geochemical features. Profiles of the sedimentological characteristics within these zones are shown in Figure 5, and are described below, starting with the bottom of the core.

**Zone I (90–78.9 cm).** The OM in this zone varies from 1.5% to 4%, with a mean of 2.6% (Figure 5b). Magnetic susceptibility is at its maximum ( $234 \times 10^{-5}$  SI) near the bottom of the core and decreases upward through the zone to reach  $38 \times 10^{-5}$  SI (Figure 5c). These high values are coupled to relatively coarse particle sizes, and abundant large grains (250–1000  $\mu\text{m}$ ) of feldspar and quartz are found sporadically in the finer matrix. These particles are presumed to be transported by wind and deposited on the lake ice cover during winter, and we refer to them as niveo-aeolian grains (Figure 5h). The sedimentary matrix in zone I is mainly composed of medium silt to fine sand ( $>60\%$  between 30 and 130  $\mu\text{m}$ ) (Figure 5d). The median grain size decreases upward through the zone from 130 to 18  $\mu\text{m}$ . The grain size distribution is poorly sorted (index of 3.2 to 4.1), but only slightly skewed ( $-0.9 < \text{skewness} < -0.1$ ), implying that the mean of the distribution is close to its median. Examination of thin sections did not reveal any remarkable sedimentary structures in this zone, other than the sporadic presence of niveo-aeolian grains (Figure 5h).

**Zone II (78.9–57.9 cm).** The relatively high sediment density in this zone, which shows as dark gray shades on the x-radiography, is linked to relatively low water content, decreasing upward from  $\sim 30\%$  to  $20\%$  (Figure 5a). Magnetic susceptibility and OM content also decrease upward (Figure 5b and c). The transition from zone I to II is clearly distinct in the particle size distribution and magnetic susceptibility graphs (Figure 5c and d). The grain size distribution shifts toward a median of  $\sim 35$   $\mu\text{m}$ , while the mean grain size varies between 22 and 45  $\mu\text{m}$  (silt  $> 75\%$ ). Except for one sample at 76 cm, the particle size distribution is symmetrical ( $-0.2 \leq \text{skewness} \leq 0.8$ ) and moderately sorted (index  $\sim 2$ ). Diffuse layers are observed in thin sections, as well as an important decrease in the number of niveo-aeolian grains relative to zone I (Figure 5h). The estimated mean sedimentation rate in zone II is  $0.23 \text{ cm a}^{-1}$  (Figure 4).

**Zone III (57.9–14.6 cm).** The x-radiography for this zone suggests a low sediment density relative to zones I and II, which also corresponds with a higher water content (27–45%) (Figure 5a). The grain size distribution in the lower part of the zone (47–57.9 cm) is variable (median between 20 and 54  $\mu\text{m}$ ) and the sedimentation rate relatively high ( $0.26 \text{ cm a}^{-1}$ ), whereas the grain size distribution is more constant from 47 to 14.6 cm (median from 26 to 38  $\mu\text{m}$ ) and the sedimentation rate is lower ( $0.10 \text{ g cm}^{-2} \text{ a}^{-1}$ ) than in underlying sediments (Figure 4). Sorting is similar to that in zone II, the index varying from 1.9 to 2.7. Apart from sporadic niveo-aeolian grains, the main distinguishing structural feature of zone III is the notable presence of *in situ* perturbation features (distorted layers) observed in the thin sections (Figure 5h).

**Zone IV (14.6–0 cm).** The OM content in zone IV decreases upward from 1.1% to 0.04% (Figure 5b). The median grain size varies between 20 and 30  $\mu\text{m}$ , which are the smallest median values in the entire core. Sediment in zone IV is mainly composed of

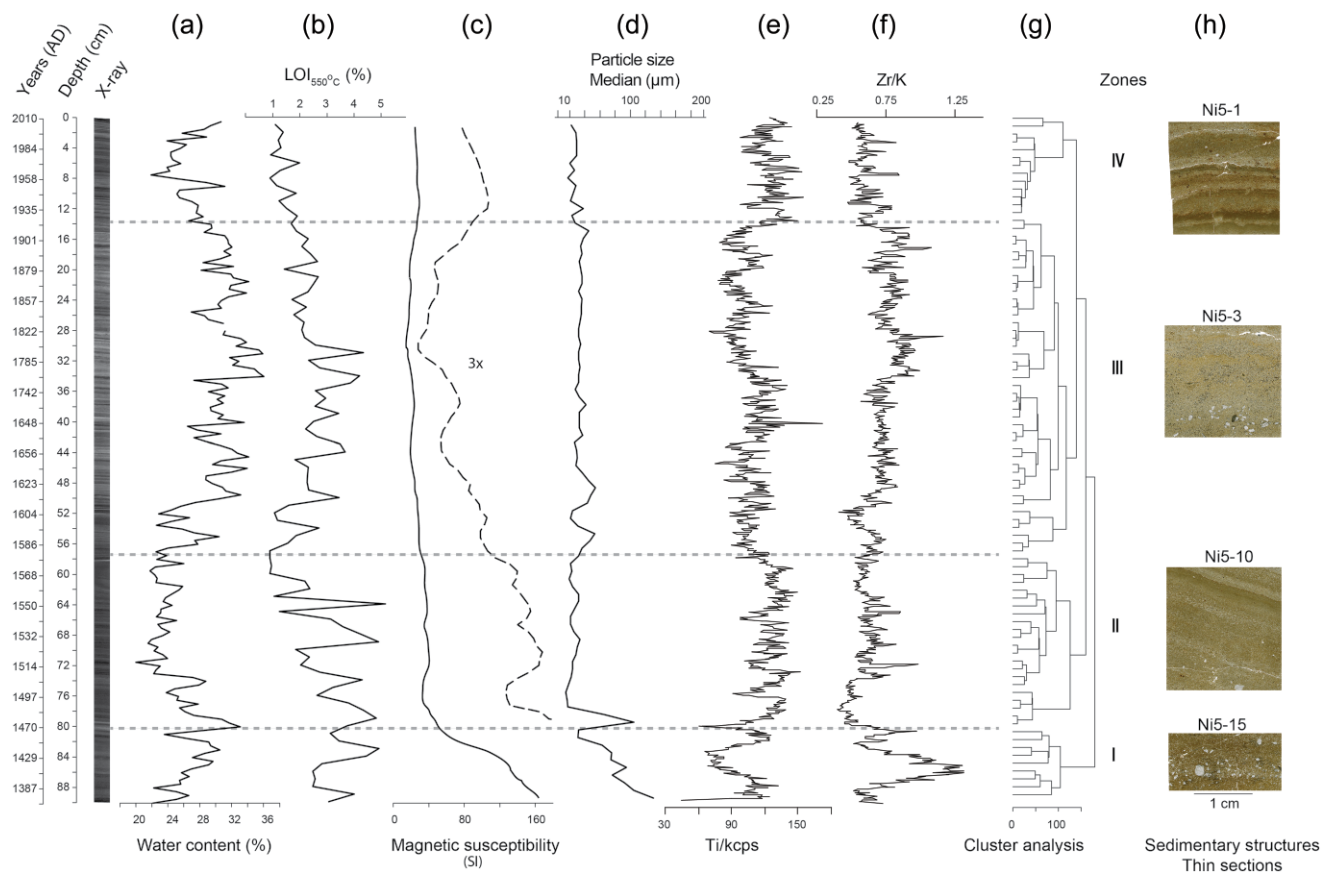


**Figure 5.** Summary diagram of Nettleing Lake core showing lithostratigraphic characteristics: (a) water content in percentage; (b) organic matter in percentage; (c) magnetic susceptibility of the core with threefold exaggeration of the abscissa to emphasize the details; (d) particle size analysis (median  $\mu\text{m}$ ); (e) Ti/kcps:  $\mu$ -XRF results from Nettleing Lake sedimentary sequence. Elemental profile in peak areas is normalized by total counts per second (kcps) at the corresponding depth. Single elemental and ratio profiles are presented with 10-point averages. Ti profile is terrigenous indicator; (f) Zr/K ratio is a proxy for particle size estimation; (g) cluster analysis revealing four stratigraphic zones; (h) typical sedimentary structures observed in thin sections.

silt at >80%. Laminations are visible in thin sections, with thickness ranging from 0.3 to 3 mm, but more commonly between 0.5 and 1.5 mm (Figure 5h). These laminations consist of alternating finer and coarser silt layers, but the irregular and disturbed nature of laminae does not allow for an unambiguous classification as varves (i.e. annual deposits). Furthermore, counting couplets of laminae from the top of the core (2010) down to the  $^{137}\text{Cs}$  peak (1963) only yielded approximately half of the expected total of 47 years. No niveo-aeolian grains were found in thin sections; however, some fecal pellets ( $\sim 0.2$ – $0.6$  mm) were observed.

### Geochemistry

A total of 27 elements were measured in core Ni5-8. However, only silicon (Si), potassium (K), calcium (Ca), titanium (Ti), iron (Fe), rubidium (Rb), strontium (Sr), and zirconium (Zr) are discussed in this paper because other elements presented noisy profiles near the limits of detection. Coefficients of correlation ( $R$ ) were computed between down-core variations in these elements in order to identify significant geochemical associations between them (Table 2). Strong positive correlations were found between Si, Ti, K, Ca, and Sr ( $0.73 \leq R \leq 0.91$ ,  $p \leq 0.01$ ,  $\alpha = 0.05$ ).

In view of the dominant lithologies in the eastern part of the Nettleing Lake watershed (granites and gneisses), we consider that these five elements are good indicators of detrital inputs into the lake.

The Si/Ti ratio is commonly used as a proxy for biogenic silica (Rothwell and Rack, 2006). However, considering the high correlation between Ti and Si ( $R = 0.73$ ,  $p \leq 0.01$ ) in core Ni5-8, the predominantly crystalline bedrock geology of the region, and the

low amount of biogenic silica (see section ‘Diatom stratigraphy’) in the sediments, it is more likely that Si concentrations in Nettleing core Ni5-8 are controlled by inorganic silica inputs.

Variations in the Zr/K ratio (Figure 5f) in the core follow those in the particle size profile. Generally, Zr is associated with weathering-resistant, coarse mineral particles such as zircon ( $\text{ZrO}_2$ ) and K with less resistant and, therefore, usually finer particles (feldspars and clay minerals); thus, the Zr/K ratio is a good proxy for relative particle size (Cuven et al., 2010), which is confirmed by the particle size distribution (Figure 5d).

### Diatom stratigraphy

The biostratigraphy of core Ni5-8 was divided into three zones of distinctive limnological features. These zones are shown in Figure 6, and are described below, starting with the bottom of the core.

Diatoms below 65 cm in core Ni5-8 are found in extremely low concentration and they are highly fragmented, presenting signs of erosion and dissolution (Figure 6). Few fragments could be identified as taxa belonging to the freshwater genera *Eunotia* spp., *Pinnularia* spp., *Frustulia* spp., *Aulacoseira* spp., and *Tabellaria* spp.

In zone A, from 65 to 47.5 cm depth, diatoms are still found at low concentration, but are less fragmented and eroded than below. Most taxa that could be identified belong to the freshwater genera *Fragilaria*, *Tabellaria*, *Eunotia*, *Brachysira* and *Pinnularia*. Diatoms appear to be better preserved in zone B, starting at 47 cm depth or AD  $\sim 1625$ . The concentration of diatoms varies from 0 to  $30.31 \times 10^5$  valves  $\text{g}^{-1}$  dry sediment. Of a total of 158 different

**Table 2.** Correlation coefficients ( $R$ ) calculated for linear regressions between geochemistry data recorded in core Ni5-8. Strong positive correlations were found between Si, Ti, K, Ca, and Sr (shaded in gray).

	Si	K	Ca	Ti	Fe	Rb	Sr	Zr
Si	I							
K	0.901	I						
Ca	0.863	0.850	I					
Ti	0.731	0.849	0.626	I				
Fe	0.377	0.477	0.134	0.603	I			
Rb	0.336	0.493	0.401	0.413	0.094	I		
Sr	0.770	0.676	0.808	0.476	0.034	0.557	I	
Zr	0.158	0.209	0.389	0.033	-0.288	0.0518	0.436	I

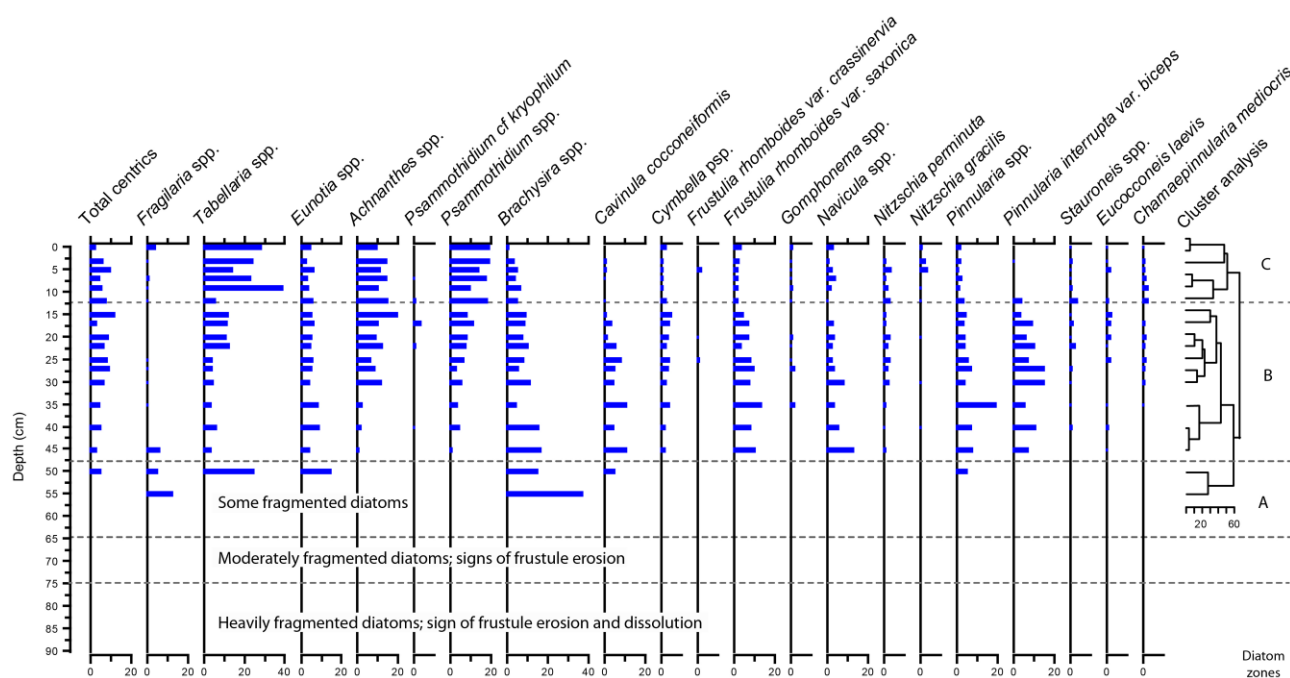


**Figure 6.** Summary biostratigraphy of diatom taxa in core Ni5-8 expressed as relative abundances (%). Only taxa with >2% abundance in at least one level are shown.

taxa identified in core Ni5-8, only 83 have relative abundances >1%, and 41 have abundances >2%. The latter represent at least 79% of the diatoms identified in each sample. Most benthic diatoms identified in this zone belong to the genera *Eunotia*, *Brachysira*, *Cavinula*, *Frustulia* and *Pinnularia*, which are typically associated with circumneutral to slightly acidic and low-electrolyte waters, as well as with dystrophic bog environments (Antoniades et al., 2008; Fallu et al., 2000; Krammer and Lange-Bertalot, 1986, 1991a, 1991b; Pienitz, 2001). Zone C (after AD~1911) is characterized by a decrease in taxa belonging to these genera and concurrent with increases in *Psammothidium* spp. and *Tabellaria flocculosa*.

## Discussion

### Nettilling Lake palaeoenvironments

**Zone I (early LIA: mid-14th century to mid/late 15th century).** The characteristics of the lowermost zone I in core Ni5-8 suggest that sedimentary processes in Nettilling Lake during the 14th and 15th centuries were completely different from those that prevailed later. Compared with the other three zones, the relatively coarse particle size and the abundance of niveo-aeolian grains are indicative of sediment inputs from proximal sources. Considering the low catchment topography, it is plausible that the drainage

network feeding into Nettilling Lake was different than at the present. A possible greater inflow of water draining the carbonate terrain in zone I, relative to zone II, is plausible, although speculative, and could explain the poor diatom frustule preservation prior to the mid/late 16th century, an observation often reported from alkaline Arctic lake sediments (Flower, 1993; Ryves et al., 2009).

**Zone II (warm phase of LIA: mid/late 15th century to mid/late 16th century).** The relatively high mean sedimentation rate ( $0.23 \text{ cm a}^{-1}$ ) and the presence of laminations throughout this zone are characteristics usually associated with warmer climatic conditions in Arctic lake sediment records (Hughen et al., 2000; Lamoureux and Gilbert, 2004; Moore et al., 2001). Some changes in sediment transfer could have occurred in the Isortoq River between zones I and II, such that discharge of silty sediment in the bay where the cores were obtained increased, thereby reducing the mean grain size (in zone II). Thomas and Briner (2009) provide evidence for a warming period during the LIA that lasted from AD 1375 to 1575 in varved sediments from Big Round Lake (northeastern Baffin Island) (Figure 7). We postulate that during this warmer interval, the rate of glacial meltwater discharge from Penny Ice Cap into the Isortoq River increased substantially, and this is indirectly supported by glaciological evidence (see section 'Comparison with the Penny Ice Cap summer melt record'). Once



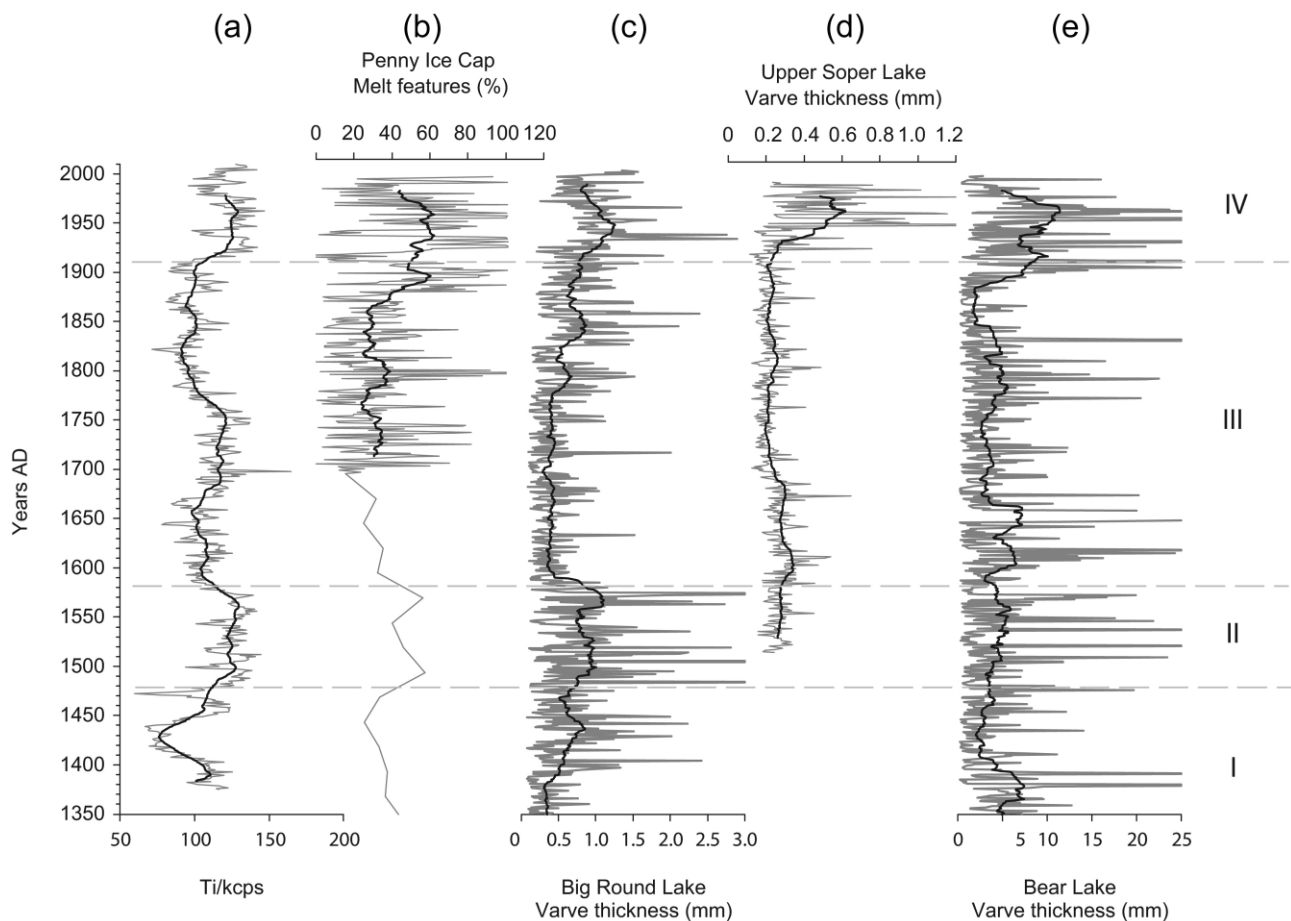


**Figure 7.** Comparison of the (a) titanium profile from the Nettilling Lake sediment record (30-year running mean) with (b) melt features from the Penny Ice Cap (Fisher et al., 1998), (c) varve thickness from Big Round Lake (Thomas and Briner, 2009), (d) varve thickness from Upper Soper Lake (Hughen et al., 2000), and (e) varve thickness from Bear Lake (Lamoureux and Gilbert (2004). Black lines are 30-year running means.

the sediment storage capacity along the Isurtuq River was exceeded, the inflow of silty glacial meltwaters into Nettilling Lake via the Isurtuq River would have increased significantly. However, this new inflow apparently did not lower lake water pH sufficiently to allow for good diatom frustule preservation.

**Zone III (late cold phase of LIA: mid/late 16th century to early 20th century).** Sediment laminations rendered visible through x-radiographs in this part of the core are not recognizable in thin sections. This may be due to some bioturbation, coupled with decreasing sedimentation rates after AD~1600 (Figure 4). With lower sedimentation rates, water circulation or small benthic organisms can more easily disturb the water–sediment interface. The abundant niveo-aolian grains found in zone III are generally associated with the presence of expanded lake ice cover, high surface wind velocities and/or reduced snow accumulation in the catchment basin (Lamoureux and Gilbert, 2004; Lewis et al., 2002). Winds capable of entraining coarse sediments such as niveo-aolian grains are usually more frequent during cold and dry climatic periods. More numerous sand particles can be trapped in cracks during a longer period when ice is covering the lake, and stronger winds also favor the formation of such lake ice cracks (Vologina et al., 2005). Lamoureux and Gilbert (2004) observed a relative increase in the abundance of coarse grains between AD 1350 and 1750 in the sedimentary record from Bear Lake (Devon Island). These considerations suggest that zone III in the Nettilling Lake Ni5-8 record is associated with a period of relatively cool, dry and windy climatic conditions, which may correspond to the coldest phase of the LIA. Sedimentary, palaeolimnological, and glaciological records indicate that in the eastern

Canadian Arctic, the LIA spanned an extended period between the 13th and 19th centuries (Briner et al., 2009; Grunet et al., 2001; Kaufman et al., 2009; Miller et al., 2012; Moore et al., 2001; Roland et al., 2009; Thomas and Briner, 2009). Moreover, compiled lichenometric ages and radiocarbon dates on fossil vegetation exhumed from beneath Canadian Arctic ice caps bracket several late Neoglacial episodes of ice cap expansion on southern Baffin Island, the latest and most extensive beginning ca. AD 1500 and ending in the mid/late 19th century (Margreth et al., 2014; Miller et al., 2012). We suggest that zone III in core Ni5-8 represents sedimentation during part of this latest interval, which was also characterized by reduced inputs of glacial meltwater into Nettilling Lake, presumably owing to colder conditions and reduced summer snow/ice melt (see also section ‘Comparison with the Penny Ice Cap summer melt record’ below). This could also explain the apparent increase in LOI in zone III, which may result from lower inputs of detrital sediment because of colder conditions and reduced meltwater inputs. We further postulate that by that time, the pH in Lake Nettilling water had dropped below 7, allowing the preservation of diatoms in the sediments. The greater diatom diversity during this period (Figure 6) likely resulted from reduced water turbidity, greater water column transparency, and stability, and hence deeper light penetration during the short summer ice-free period in the lake and the Isurtuq River. The diatom accumulation rate might not be highest during zone III, as increased absolute diatom abundance values during this zone may be a function of reduced sediment inputs (as reflected by higher LOI). The diatom assemblage found in this zone is mostly composed of benthic circumneutral to acidophilic taxa (e.g. *Brachysira procera*, *Cavinula cocconeiformis*, *Frustulia saxonica* and *Pinnularia* spp.) that are usually found in wetlands rich in

*Sphagnum* moss habitats (Antoniades et al., 2008; Fallu et al., 2000; Krammer and Lange-Bertalot, 1986, 1991a, 1991b; Pienitz, 2001). Thus, their abundance could reflect the presence of extensive moss mats that may have covered the banks of the Isurtuq River at a time of reduced inflow (Figure 2).

**Zone IV (after the early 20th century).** The abrupt transition from zones III to IV in core Ni5-8 indicates that conditions in Nettilling Lake changed markedly in the early 20th century. These changes are reflected in many sediment properties such as grain size, magnetic susceptibility and diatom assemblage composition (Figures 5 and 6). The mean sedimentation rate in the lake had apparently increased earlier, possibly as early as the mid-19th century (Figure 4). This timing agrees well with the inferred termination of the LIA as documented in other regional proxy records (Margreth et al., 2014; Rolland et al., 2009). Rising temperatures would have caused increased seasonal snow and ice melt rates and detrital sediment delivery into the lake (see also section 'Comparison with the Penny Ice Cap summer melt record'). Positive correlations between air temperature and sedimentation rates have been documented in several Canadian Arctic lakes (Hughen et al., 2000; Lamoureux and Gilbert, 2004; Moore et al., 2001). Rapid sedimentation flux reduces the potential for bioturbation and may explain the better preservation of laminated sediment structures in the upper part of the Nettilling Lake core Ni5-8. It is also noteworthy that the increase in Ti concentration in the core in the early 20th century coincides, within possible dating errors, with a marked increase in the thickness of varves in the sediment records of Upper Soper Lake (southern Baffin Island; Hughen et al., 2000), Bear Lake (Devon Island; Lamoureux and Gilbert, 2004), and Big Round Lake (eastern Baffin Island; Thomas and Briner, 2009), reflecting a rise in regional air temperatures (Figure 6). The changes observed in floral composition in core Ni5-8 closely mirror those displayed in the sedimentological and geochemical proxies. More competitive genera, such as *Tabellaria*, *Achnanthes* and *Psammothidium*, progressively replaced the benthic acidophilic taxa found before the 20th century, probably because of reduced light penetration in Nettilling Lake as silty meltwater inflows from Penny Ice Cap increased via the Isurtuq River.

#### Comparison with the Penny Ice Cap summer melt record

To further investigate the hydrological connection between sedimentation in eastern Nettilling Lake and glacial melt rates on southern Baffin Island, we compared the profile of Ti abundance obtained from core Ni5-8 with a proxy record of past summer warmth developed from ice cores drilled at the summit of Penny Ice Cap (67.25°N, 65.77°W, ~1860 m a.s.l.) in 1995 and 2010 (Fisher et al., 2011; Grumet et al., 2001; Zdanowicz et al., 2012). The proxy used is the volumetric percentage of 'melt features' (MF%) in the cores, which are distinct, bubble-poor layers or lenses of ice formed by the refreezing of surface meltwater into underlying firn. Koerner (1977) first established that the relative abundance of these features is correlated to past summer warmth conditions. The composite MF record developed from Penny Ice Cap cores covers the period AD 1695 to 1992 at 5 to 10-year resolution and extends to ~3300 years ago, but with a 25-year resolution only. For the period considered in this paper, that is the past six centuries, the possible dating error in the Penny Ice Cap chronology is estimated to be <10% of true age (Zdanowicz et al., 2012).

To facilitate comparison of multi-decadal trends, the time series of Ti abundance in core Ni5-8 and the Penny Ice Cap MF record were both smoothed with a 30-year running mean. This was done in part to mitigate the possible time-averaging effect of deep water percolation on the Penny Ice Cap MF% record, which may result in the apparent age of MF variations in this record

being earlier (younger) than the variations in summer warmth that caused them. Given that the summit of Penny Ice Cap, where the MF% record was developed, is situated more than 1830 m above the Nettilling Lake basin (~30 m a.s.l.), some altitude-dependent time lag may also be expected between the responses of the ice cap summit and the lake to regional temperature changes.

The smoothed time series of Ti content in Nettilling Lake core Ni5-8 and of MF% on Penny Ice Cap were found to correlate positively over the common interval AD 1695–1992 ( $R=0.45$ ,  $p=0.0579$ ,  $\alpha=0.05$ ), with the strength of the correlation increasing after the mid-19th century ( $R=0.63$ ,  $p=0.011$ ; Figure 7a and b). The earlier part of the Penny Ice Cap MF%, although with a limited 25-year resolution, also shows a general agreement with the pattern of variations seen in the Nettilling Lake Ti record from mid-14th century to late 17th century. The good correspondence between these two records supports our hypothesis that changes in Ti concentrations in sediments of eastern Nettilling Lake are modulated, on multi-decadal to secular time scales, by the supply of silty glacial meltwater from Penny Ice Cap via the Isurtuq River. During colder periods associated with reduced summer Penny Ice Cap melt rates, the supply of fine glacial sediments to the lake is presumably reduced, whereas during periods of increased summer melt rates the supply of these sediments to the lake increases.

Some secular changes in melt rates of Penny Ice Cap appear to be offset by a few decades relative to the presumed corresponding changes in Ti abundance in core Ni5-8. For example, the initial rise in MF% of Penny Ice Cap at the end of the LIA occurred between AD ~1860 and 1890, whereas Ti concentrations in eastern Nettilling Lake sediments increased later, at AD 1900 or later. The mismatch could be due to age model inaccuracies in one or the other (or both) records (see Figure 4). It could also imply that melt rates on Penny Ice Cap must exceed some threshold for a sedimentological response to be registered in the Nettilling Lake sediment record. This threshold might conceivably vary over time as a function of the channel morphology, sediment storage capacity, and drainage configuration of the Isurtuq River, as discussed earlier.

## Summary and conclusion

Using multiple proxies, we developed a ~600-year long, high-resolution palaeoenvironmental record from a sediment core taken in Nettilling Lake on Baffin Island, at the center of a vast and remote understudied region of the Canadian Arctic Archipelago. We used an unconventional approach in palaeolimnology to establish the core chronology by combining radiometric ( $^{137}\text{Cs}$ ) and palaeomagnetic dating techniques, which allowed us to date the bottom of the 90-cm long core to the mid-14th century. This finding implies a relatively high mean sedimentation rate (~0.15 cm a<sup>-1</sup>) for an Arctic lake.

Our sedimentary record from Nettilling Lake spans most of the LIA cold interval (mid-13th to 19th centuries). It contains evidence for at least two episodes of colder and drier conditions during this period (mid-14th century to mid/late 15th century and mid/late 16th century to early 20th century), with somewhat warmer conditions in between. The second cool interval is presumed to correspond with the coldest phase of the LIA in this region. At the turn of the 20th century, major shifts observed in all proxies were interpreted as reflecting the impact of recent climate warming in this region. At the same time, we noticed a shift toward more clearly defined sediment laminations, decreasing particle size, as well as important changes in diatom community composition.

Down-core variations of Ti in the sediments were compared with independent reconstructions of regional summer temperatures derived from ice core and varved lake sediment records from Baffin Island. These comparisons revealed significant positive correlations, thereby emphasizing the usefulness of combining geochemical and

biostratigraphic proxies in palaeolimnological studies. Further research on the Nettilling Lake sediment archive promises to yield more detailed insights into the climatic and environmental history of this poorly known region of the Canadian Arctic.

### Acknowledgements

Implementation of the Iterative Amplitude Adjusted Fourier Transform (IAAFT) algorithm for estimating age model errors was facilitated by using MATLAB codes developed and made available by A Leontitis and V Venema. We would like to thank GH Miller and an anonymous reviewer for their insightful comments on an earlier version of the manuscript.

### Funding

This study was made possible through grants from the Natural Sciences and Engineering Research Council (NSERC) of Canada to R Pienitz, P Francus, G St-Onge and from the Network of Centres of Excellence *ArcticNet*. The Polar Continental Shelf Program (PCSP), the Northern Studies Training Program (NSTP), and Centre d'Études Nordiques (CEN) provided logistic support for the fieldwork at Nettilling Lake.

### References

- Antoniades D, Francus P, Pienitz R et al. (2011) Holocene dynamics of the Arctic's largest ice shelf. *Proceedings of the National Academy of Sciences of the United States of America* 108(47): 18899–18904.
- Antoniades D, Hamilton PB, Douglas MSV et al. (2008) Diatoms of North America: The freshwater floras of Prince Patrick, Ellef Ringes, and Northern Ellesmere Islands from the Canadian Arctic Archipelago. In: Lange-Bertalot H (ed.) *Iconographia Diatomologica*, vol. 17. Ruggell: A.R.G. Gantner Verlag KG, 649 pp.
- Appleby P (2001) Chronostratigraphic techniques in recent sediments. In: Last WM and Smol JP (eds) *Tracking Environmental Change Using Lake Sediments: Basin Analysis, Coring and Chronological Techniques* (Development in Palaeoenvironmental Research (DPER)). Dordrecht: Springer, pp. 171–203.
- Axford Y, Briner JP, Cooke CA et al. (2009) Recent changes in a remote Arctic lake are unique within the past 200,000 years. *Proceedings of the National Academy of Sciences* 106(44): 18443–18446.
- Barletta F, St-Onge G, Channell JET et al. (2010a) Dating of Holocene western Canadian Arctic sediments by matching palaeomagnetic secular variation to a geomagnetic field model. *Quaternary Science Reviews* 29: 2315–2324.
- Barletta F, St-Onge G, Stoner SJ et al. (2010b) A high-resolution Holocene palaeomagnetic secular variation and relative palaeointensity stack from Eastern Canada. *Earth and Planetary Science Letters* 298: 162–174.
- Battarbee R, Jones V, Flower R et al. (2002) Diatoms. In: Smol J, Birks J, Last W et al. (eds) *Tracking Environmental Change Using Lake Sediments: Terrestrial, Algal, and Siliceous Indicators* (Development in Palaeoenvironmental Research (DPER)). Dordrecht: Springer, pp. 155–202.
- Birks HJB (2012) Analysis of stratigraphical data. In: Birks HJB, Lotter AF, Juggings S et al. (eds) *Tracking Environmental Change Using Lake Sediments: Data Handling and Numerical Techniques* (Development in Palaeoenvironmental Research (DPER)). Dordrecht: Springer, pp. 355–378.
- Blaauw M and Christen JA (2011) Flexible paleoclimate age-depth models using an autoregressive gamma process. *Bayesian Analysis* 6: 457–474.
- Blackadar RG (1967) Geological reconnaissance, southern Baffin Island, District of Franklin. *Geological Survey of Canada Paper* 66(47): 32 p.
- Blake W, Jr (1966) End moraines and deglaciation chronology in northern Canada with special reference to southern Baffin Island. *Geological Survey of Canada Paper* 66(26): p. 31.
- Blott S and Pye K (2001) GRADISTAT: A grain size distribution and statistics package for the analysis of unconsolidated sediments. *Earth, Surface, Processes and Landforms* 26(11): 1237–1248.
- Briner JP, Davis TP and Miller GH (2009) Latest Pleistocene and Holocene glaciation of Baffin Island, Arctic Canada: Key patterns and chronologies. *Quaternary Science Reviews* 28: 2075–2087.
- Cook TL, Bradley RS, Stoner JS et al. (2009) Five thousand years of sediment transfer in a high arctic watershed recorded in annually laminated sediments from Lower Murray Lake, Ellesmere Island, Nunavut, Canada. *Journal of Paleolimnology* 41: 77–94.
- Croudace IW, Rindby A and Rothwell RG (2006) ITRAX: Description and evaluation of a new sediment core scanner. In: Rothwell RG (ed.) *New Ways of Looking at Sediment Cores and Core Data*. London: Geological Society of London (Special Publication), pp. 51–63.
- Cuven S, Francus P and Lamoureux S (2010) Estimation of grain size variability with micro X-ray fluorescence in laminated lacustrine sediments, Cape Bounty, Canadian High Arctic. *Journal of Paleolimnology* 44: 803–817.
- Dyke (1979) Glacial and Sea-Level History of Southwestern Cumberland Peninsula, Baffin Island, N.W.T., Canada. *Arctic, Antarctic and Alpine Research* 11(2): 179–202.
- Ebisuzaki W (1997) A method to estimate the statistical significance of a correlation when the data are serially correlated. *Journal of Climate* 10: 2147–2153.
- Everett JT and Fitzharris BB (1998) The Arctic and the Antarctic. In: Watson RT, Zinyowera MC, Moss RH et al. (eds) *The Regional Impacts of Climate Change. An Assessment of Vulnerability* (A special report of IPCC working group II for the Intergovernmental Panel of Climate Change). Cambridge: Cambridge University Press, pp. 85–103.
- Fallu MA, Allaire N and Pienitz R (2000) *Freshwater Diatoms from Northern Québec and Labrador (Canada): Species-Environment Relationships in Lakes of Boreal Forest, Forest-Tundra and Tundra Regions*. Berlin: Cramer, 200 pp.
- Fisher D, Zheng J, Burges D et al. (2011) Recent melt rates of Canadian Arctic ice caps are the highest in four millennia. *Global and Planetary Change* 84–85: 3–7.
- Fisher DA, Koerner RM, Bourgeois J et al. (1998) Penny Ice Cap cores, Baffin Island, Canada, and the Wisconsin Foxe Dome connection: Two states of Hudson Bay ice cover. *Science* 279: 692–695.
- Flower RJ (1993) Diatom preservation: Experiments and observations on dissolution and breakage in modern and fossil material. *Hydrobiologia* 269(270): 473–484.
- Grumet NS, Wake CP, Mayewski PA et al. (2001) Variability of sea ice in Baffin Bay over the last millennium. *Climatic Change* 49: 129–145.
- Heiri O, Lotter A and Lemcke G (2001) Loss on ignition as a method for estimating organic and carbonate content in sediments: Reproducibility and comparability of results. *Journal of Paleolimnology* 25: 101–110.
- Hodgson DA and Smol JP (2008) High-latitude palaeolimnology. In: Vincent WF and Laybourn-Parry J (eds) *Polar Lakes and Rivers: Limnology of Arctic and Antarctic Aquatic Ecosystems*. Oxford: Oxford University Press, pp. 43–64.
- Hughen K, Overpeck J and Anderson R (2000) Recent warming in the 500-year palaeotemperature record from varved sediments, Upper Soper Lake, Baffin Island, Canada. *The Holocene* 10: 9–19.

- Jackson A, Jonkers ART and Walker MR (2000) Four centuries of geomagnetic secular variation from historical records. *Philosophical Transaction of Royal Society of London* 358: 957–990.
- Jacobs JD, Headley AN, Maus LA et al. (1997) Climate and vegetation of the Interior Lowlands of Southern Baffin Island: Long-term stability at the low arctic limit. *Arctic* 50(2): 167–177.
- Kaufman DS, Schneider DP, McKay NP et al. (2009) Recent warming reverses long-term Arctic cooling. *Science* 325: 1236–1239.
- Koerner RM (1977) Devon Island ice cap: Core stratigraphy and palaeoclimate. *Science* 196: 15–18.
- Korte M and Constable C (2011) Improving geomagnetic field reconstructions for 0–3 ka. *Physics of the Earth and Planetary Interiors* 188: 247–259.
- Krammer K and Lange-Bertalot H (1986) Bacillariophyceae 1. Teil: Naviculaceae. In: Ettl H, Gerloff J, Heynig H et al. (eds) *Süßwasserflora von Mitteleuropa*, Band 2/1. Stuttgart: Gustav Fischer Verlag, 876 pp.
- Krammer K and Lange-Bertalot H (1988) Bacillariophyceae 2. Teil: Bacillariaceae, Epithemiaceae, Surirellaceae. In: Ettl H, Gerloff J, Heynig H et al. (eds) *Süßwasserflora von Mitteleuropa*, Band 2/2. Stuttgart: Gustav Fischer Verlag, 596 pp.
- Krammer K and Lange-Bertalot H (1991a) Bacillariophyceae 3. Teil: Centrales, Fragilariaceae, Eunotiaceae. In: Ettl H, Gerloff J, Heynig H et al. (eds) *Süßwasserflora von Mitteleuropa*, Band 2/3. Stuttgart: Gustav Fischer Verlag, 576 pp.
- Krammer K and Lange-Bertalot H (1991b) Bacillariophyceae 4. Teil: Achnanthaceae, Kritische Ergänzungen zu Navicula (Lineolatae) und Gomphonema Gesamtliteraturverzeichnis Teil 1–4. In: Ettl H, Gerloff J, Heynig H et al. (eds) *Süßwasserflora von Mitteleuropa*, Band 2/4. Stuttgart: Gustav Fischer Verlag, 436 pp.
- Lamoureux SF (1994) Embedding unfrozen lake sediments for thin section preparation. *Journal of Paleolimnology* 10(2): 141–146.
- Lamoureux SF and Gilbert R (2004) A 750-yr record of autumn snowfall and temperature variability and winter storminess recorded in the varved sediments of Bear Lake, Devon Island, Arctic Canada. *Quaternary Research* 61: 134–147.
- Lewis T, Gilbert R and Lamoureux SF (2002) Spatial and temporal changes in sedimentary processes at proglacial bear lake, Devon Island, Nunavut, Canada. *Arctic, Antarctic and Alpine Research* 34(2): 119–129.
- Margreth A, Dyke AS, Gosse JC et al. (2014) Neoglacial ice expansion and Late-Holocene cold-based ice cap dynamics on Cumberland, Peninsula, Baffin Island, Arctic Canada. *Quaternary Science Reviews* 91: 242–256.
- Mazaud A (2005) User-friendly software for vector analysis of the magnetization of long sediment cores. *Geochemistry, Geophysics, Geosystems* 6(12): 1–5.
- Miller GH, Geirsdóttir A, Zhong Y et al. (2012) Abrupt onset of the Little Ice Age triggered by volcanism and sustained by sea-ice/ocean feedbacks. *Geophysical Research Letters* 39: L02708.
- Miller GH, Lehman SJ, Refsnider KA et al. (2013) Unprecedented recent summer warmth in Arctic Canada. *Geophysical Research Letters* 40: 5745–5751.
- Moore GWK (2006) Reduction in seasonal sea ice concentration surrounding southern Baffin Island 1979–2004. *Geophysical Research Letters* 33(20): 1–5.
- Moore JJ, Hughen KA, Miller GH et al. (2001) Little Ice Age recorded in summer temperature reconstruction from varved sediments of Donard Lake, Baffin Island, Canada. *Journal of Paleolimnology* 25: 503–517.
- Narancic B, Chaplignin B, Meyer H et al. (2013) Postglacial environmental succession of Nettiilling Lake (Baffin Island, Canadian Arctic) inferred by biogeochemical and microfossil proxies. In: *European geosciences union general assembly 2013*, Vienne, 7–12 April.
- Oliver DR (1964) A limnologic investigation of a large Arctic lake, Nettiilling Lake, Baffin Island. *Arctic* 17(2): 69–83.
- Overpeck J, Hughen K, Hardy D et al. (1997) Arctic environmental change of the last four centuries. *Science* 278: 1251–1256.
- Paillard (2006) *AnalySerie Software*. Available at: <http://www.lsce.ipsl.fr/Phoccea/Page/index.php?id=3> (accessed 22 September 2014).
- Pienitz R (2001) Techniques de Reconstitution du Développement des Tourbières: Analyse des Diatomées. In: Payette S and Rochefort L (eds) *Écologie des Tourbières du Québec-Labrador*. Québec City: Presses de l'Université Laval, pp. 311–326.
- Pienitz R, Douglas MSV and Smol JP (2004) Palaeolimnological research in polar regions: An introduction. In: Pienitz R, Douglas MSV and Smol JP (eds) *Long-Term Environmental Change in Arctic and Antarctic Lakes* (Development in Palaeoenvironmental Research (DPER)). Dordrecht: Springer, pp. 1–12.
- Rolland N, Larocque I, Francus P et al. (2009) Evidence for a warm period during the 12th and 13th centuries AD from chironomid assemblages in Southampton Island, Nunavut, Canada. *Quaternary Research* 72: 27–37.
- Rothwell G and Rack F (2006) New techniques in sediment core analysis: An introduction. In: Rothwell G (ed.) *New Techniques in Sediment Core Analysis*. London: Geological Society of London (Special Publications 267), pp. 1–29.
- Ryves DB, Battarbee RW and Fritz SC (2009) The dilemma of disappearing diatoms: Incorporating diatom dissolution data into palaeoenvironmental modeling and reconstruction. *Earth and Atmospheric Science* 128: 120–136.
- Schreiber T and Schmitz A (1996) Improved surrogate data for nonlinearity tests. *Physical Review Letters* 77: 635–638.
- Stoner JS and St-Onge G (2007) Magnetic stratigraphy in paleoceanography: Reversals, excursions, palaeointensity and secular variation. In: Hillaire-Marcel C and De Vernal A (eds) *Proxies in Late Cenozoic Paleoclimatology*. Amsterdam: Elsevier, pp. 99–137.
- St-Onge G and Stoner JS (2011) Paleomagnetism near the North Magnetic Pole: A unique vantage point to understand the dynamics of the geomagnetic field and its secular variations. *Oceanography* 24: 42–50.
- St-Onge MR, Wodicka N and Ijewliw O (2007) Polymetamorphic evolution of the Trans-Hudson Orogen, Baffin Island, Canada: Integration of petrological, structural and geochronological data. *Journal of Petrology* 48: 271–302. doi:10.1093/petrology/eg1060.
- Tauxe L (2010) *Essentials of Palaeomagnetism*. Berkeley, CA: University of California Press, 489 pp.
- Thomas EK and Briner JP (2009) Climate of the past millennium inferred from varved proglacial lake sediments on northeast Baffin Island, Arctic Canada. *Journal of Paleolimnology* 49: 209–224.
- Vologina EG, Granin NG, Vorobeva SS et al. (2005) Ice-rafting of sand-silt material in South Baikal. *Russian Geology and Geophysics* 46(4): 420–427 (in Russian).
- Wolfe A and Smith R (2004) Palaeolimnology of the middle and high Canadian Arctic. In: Pienitz R, Douglas MSV and Smol JP (eds) *Long-Term Environmental Change in Arctic and Antarctic Lakes* (Development in Palaeoenvironmental Research (DPER)), vol. 8, issue 9. Dordrecht: Springer, pp. 241–268.
- Zdanowicz C, Smetny-Sowa A, Fisher D et al. (2012) Summer melt rates on Penny Ice Cap, Baffin Island: Past and recent trends and implications for regional climate. *Journal of Geophysical Research* 117(F02006): 21 pp.